

Effect of low-level laser therapy on bone repair: a randomized controlled experimental study

Valéria Regina Gonzalez Sella · Fernando Russo Costa do Bomfim ·
Paula Carolina Dias Machado · Maria José Misael da Silva Morsoleto ·
Milton Chohfi · Helio Plapler

Received: 23 September 2014 / Accepted: 5 January 2015 / Published online: 18 January 2015
© Springer-Verlag London 2015

Abstract The aim of this study was to investigate the effect of low-level laser therapy (LLLT) on bone repair in femoral fractures. Sixty adult Wistar rats were randomly assigned into one of two groups: group A (osteotomy + LLLT) or group B (osteotomy + sham laser). An experimental model of complete bone fracture was surgically created by removing a 2-mm fragment from the middle third of the femoral shaft. Data were analyzed on days 8, 13, and 18 after the fracture (subgroups 1, 2, and 3). Samples were assessed for changes in inflammatory infiltration; trabecular bone matrix, periosteal, and new bone formations; and changes in the expression of particular osteogenic-related proteins (osteocalcin, osteopontin, and osteonectin). Microscopic analysis revealed a significant decrease in inflammatory infiltration, intense trabecular bone matrix and periosteal formation, and an increase in newly formed bone after laser irradiation. We also found an increase in the expression of bone matrix proteins with LLLT, with a significant difference measured for osteocalcin in the LLLT group at day 8 ($p=0.007$). We show that LLLT plays an important role in augmenting bone tissue formation, which is relevant to fracture healing. LLLT may therefore be indicated as an adjunct therapeutic tool in clinical practice for the treatment or recovery of nonunion injuries.

Keywords Bone remodeling · Femoral fracture · Low-level laser therapy

Introduction

According to the World Health Organization, there are more than 150 diseases and syndromes related to skeletal and joint problems [1]. Approximately six million long-bone fractures are reported annually in the USA. Although progress has been made in treatment methods over the past decades, approximately 5–10 % of fractures still result in delayed union or nonunion. Moreover, 600,000 individuals experience prolonged pain and discomfort associated with fracture nonunion every year [2–6]. Among the efforts aimed at minimizing these complications, clinical solutions using energy emission (ultrasound, electrical stimulation, and laser irradiation) have been investigated [2, 5, 7]. Laser therapy is accessible, does not require the concomitant use of drugs, does not promote thermal damage to the tissue [1], and may be applied in the presence of the types of metal devices [4] commonly used to stabilize open or displaced fractures. Thus, various experimental studies have sought to define the role of low-level laser therapy (LLLT) in fracture healing [1, 3, 8, 9].

The investigation of bone formation and resorption processes involves the identification of products that are synthesized by osteoblasts and osteoclasts [10]. Noncollagenous proteins found in the organic matrix of bone tissue (osteocalcin, osteopontin, and osteonectin) are commonly used as bone mineralization markers. Because the exact mechanisms involved in the healing process of laser-irradiated bone tissues have yet to be elucidated and there are no standardized protocols for LLLT research, we sought to investigate both of these issues in an *in vivo* model and analyze the results through microscopy and immunohistochemistry. Therefore,

V. R. G. Sella · F. R. C. do Bomfim · P. C. D. Machado ·
M. J. M. da Silva Morsoleto · H. Plapler
Department of Surgery, Division of Operative Technique and
Experimental Surgery, Universidade Federal de São Paulo [Federal
University of São Paulo] – UNIFESP, São Paulo, SP, Brazil

M. Chohfi
Department of Orthopedics, Universidade Federal de São Paulo
[Federal University of São Paulo] – UNIFESP, São Paulo, SP, Brazil

V. R. G. Sella (✉)
R. Botucatu, 740, São Paulo, SP, Brazil CEP 04023-900
e-mail: valsella@uol.com.br

the aim of this study was to verify the effect of LLLT on bone repair at the interface of a nonunion femoral fracture (simulated by osteotomy) by measuring changes in major bone matrix proteins that are associated with bone formation.

Materials and methods

Group allocations

Sixty adult (12 weeks, 350 g) male Wistar rats were provided with regular standard rat food and water ad libitum throughout the experiment and were housed one animal per cage in a room with a 12-h light–dark cycle. The rats were randomly assigned into one of two groups: group A ($n=30$), or the LLLT group (osteotomy + LLLT), and group B ($n=30$), or the sham group (osteotomy + laser irradiation simulation). The rats in these groups were respectively divided into three subgroups (1–3) according to the day of death after surgery: at day 8 (subgroup 1), day 13 (subgroup 2), and day 18 (subgroup 3): A1/B1 ($n=20$), A2/B2 ($n=20$), and A3/B3 ($n=20$).

Surgery

Rats were anesthetized with a mixture of 0.4 mL of 10 % ketamine (114 mg/kg), 0.2 mL of 2 % xylazine (11.4 mg/kg), and 0.1 mL of fentanyl citrate (1.4 mg/kg) by intramuscular injection. Rats were then placed securely on the operating table in the ventral decubitus position. An incision was first made through the skin and subcutaneous tissue in the anterolateral region of the right thigh. The fascia was then opened, and the femur was accessed at the space between the *rectus femoris* and the *vastus lateralis* muscles. The middle third of the femoral shaft was exposed and a straight titanium plate (22 mm×3 mm×0.5 mm) with central space and four holes (Synthes Ind., Rio Claro, Brazil) was fixed to it with 1.5- and 1.7-mm stardrive cortex screws, according to the femur diameter. The bone was sectioned using an oscillating saw (Implantek Lase, DMC Equipment, São Carlos, Brazil) at 500–800 rpm, with continuous irrigation with saline solution to the site. An experimental model of complete bone fracture was created by removing a 2-mm fragment from the middle third of the femoral shaft (Fig. 1). A precision pachymeter was used to measure the size of the gap to ensure the distance between the fragments. After fracture creation, the muscles were approximated and the skin was closed with continuous sutures. Enrofloxacin (30 drops) was added to the rats' drinking water daily. Analgesics were not administered and splint elements were not used.

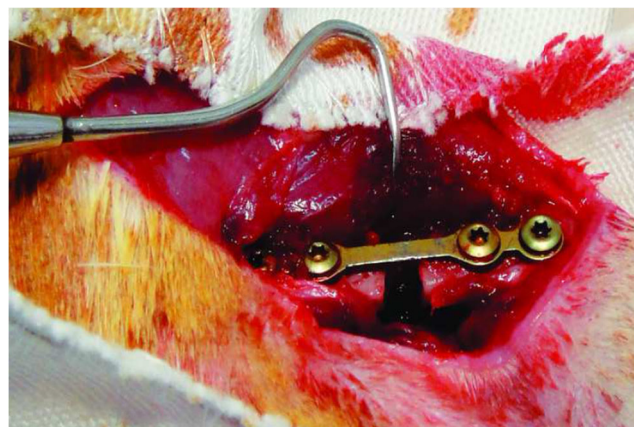


Fig. 1 Aspect of the femur after osteotomy and plate fixation

Low-level laser therapy

Rats in group A were exposed to LLLT once daily (from day 1 through day 8 after surgery) using a gallium aluminum arsenide laser device (model Magnus Plus, DMC Equipment) by direct contact to the skin at two points on the inner side of the right hind limb. The device was set according to the following parameters: continuous mode, $\lambda=808$ nm, power density of 0.2 W/cm², fluency of 37 J/cm² per site, nominal dose of 2 J, spot size of 0.02 mm², energy per point=1 J, and exposure time of 5 s per site. For exposure, each rat was positioned (Fig. 2) at its back without any restraints and placed in the hand of one of the experimenters, and the laser was applied on the opposite side of a fixed plate. The animals of group B were

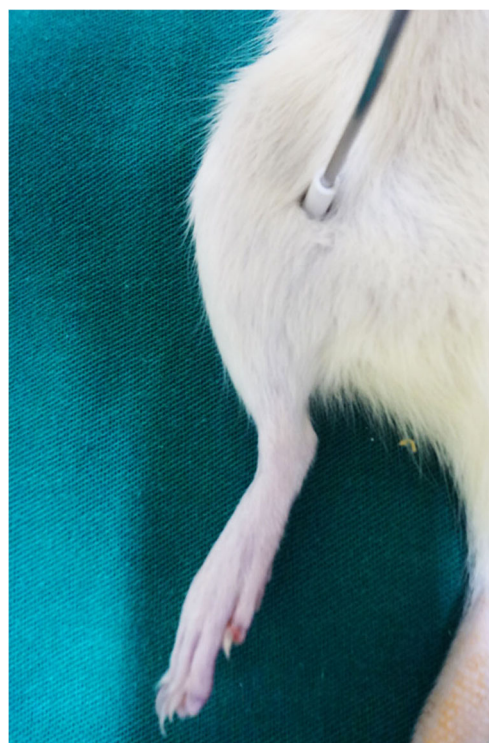


Fig. 2 Rat exposure to LLLT procedure

similarly prepared; however, they were treated with a sham laser.

On determined days, the animals were sacrificed by injection of lethal dose of anesthetics.

Microscopic analysis

Bone tissue samples were fixed in a 10 % formalin solution for 24 h. They were then individually immersed into a rapid decalcifier (0.7 g of tetrasodium EDTA, 0.14 g of sodium tartrate, 5 g of sodium/potassium tartrate; 120 mL of hydrochloric acid; 900 mL of distilled water) until total decalcification was achieved, and the samples were then washed in running water. Samples were then successively dehydrated in 70, 80, 90, and 100 % alcohol, cleared in an alcohol/xylene bath (1:1) and then in xylene until translucent. Samples were then paraffin-embedded to obtain a tissue block, cut into 6- μ m-thick sections using a Microtome (Leica Microsystems, Wetzlar, Germany), and stored in a drying oven for later staining.

Histological sections were stained with hematoxylin-eosin, examined using optical microscopy, and evaluated via image digitization and computational analysis (Image-Pro Plus version 6.3.1, Media Cybernetics, Inc., Rockville, MD, USA). Inflammatory infiltration and trabecular bone matrix formation were examined across five quadrants (four peripheral quadrants and one central quadrant) on each slide at a magnification of $\times 1000$. New bone formation was assessed using osteocyte counting within the same five quadrants in each slide at $\times 100$ magnification. A score from 0 to 4 according to the presence of characteristic cells was used to evaluate inflammatory infiltration, trabecular bone matrix, and new bone formation, where 0=none (no characteristic cells), 1=minimal (range 1–65 characteristic cells), 2=mild (range 66–135 characteristic cells), 3=moderate (range 136–200 characteristic cells), and 4=intense (>200 characteristic cells). Periosteal growth was determined as the presence or absence of the tissue found on each slide, for each animal.

Immunohistochemistry

Cross sections (6 μ m) of the cut edges of the fracture site were placed on silanized slides, fixed, deparaffinized, and incubated in sodium citrate buffer (0.01 M; pH 6.0) for antigen retrieval. Sections were then washed with phosphate-buffered saline (PBS) and immersed in methanol with 0.3 % hydrogen peroxide for endogenous peroxidase blocking. Sections were again washed with PBS and then incubated with one of three primary antibodies: anti-osteocalcin polyclonal antibody, diluted 1:250 (Santa Cruz Biotechnology, Dallas, TX, USA) [11]; anti-osteopontin monoclonal antibody, diluted 1:250 (Santa Cruz Biotechnology) [12], or anti-osteonection monoclonal antibody, diluted 1:250 (Santa Cruz Biotechnology)

[13]. All antibodies were diluted in 0.01 M PBS with 1 % bovine serum albumin for 18 h at 4 °C. After this first incubation, the sections were washed three times with PBS and then incubated with a biotinylated secondary antibody solution provided in the Universal LSAB+ Kit/HRP, Rabbit/Mouse Kit (code KO675, Dako, Glostrup, Denmark). Sections were washed and then incubated with streptavidin-biotin-peroxidase complex solution and working substrate-chromogen solution both provided in the kit, with three PBS washes in between these two steps. Finally, the sections were washed with distilled water, counterstained with 5 % methyl green, washed again with distilled water, dehydrated, and mounted in Entellan[®] (Merck Millipore, Darmstadt Germany). All immunohistochemical reactions occurred in a light-protected environment.

Immunostaining was assessed using light microscopy (Leica Microsystems), and the obtained images were analyzed using Image-Pro Plus. The intensity of the expression of proteins associated with bone formation was defined according to a score from 0 to 3 (0=no reddish-brown color, 1=light color (color code X156), 2=medium intense color (color code E118), and 3=intense color (color code R121) (<http://www.suvinil.com.br/pt/familias/2/600/tijolo.aspx>) [14]. Analysis was performed across five fields of view from each slide, and a positive control for each antibody was used to ascertain staining. This positive control staining was performed in specific cells/tissues: kidney tissue for osteocalcin and osteopontin, and lung carcinoma cells for osteonection [11–13]. The colorimetric method was compared against a standard scale. This method is well established in the literature [15, 16].

All slides for either microscopic and immunohistochemical evaluation were examined in duplicate by a biomedical professional without prior knowledge of the aim of the study.

Statistical analysis

Mann–Whitney and Kruskal–Wallis nonparametric tests were performed to determine statistical significance between groups A and B and among the subgroups ($p < 0.05$).

Results

With regard to microscopic parameters (Fig. 3), better results were found for group A than for group B (Fig. 4a, b). The fracture sites from all rats sacrificed at day 8 (subgroups A1 and B1) showed similar degrees of inflammatory infiltration, whereas only the rats of subgroup A2 (on day 13) showed a significantly lowered inflammatory infiltration response ($p = 0.015$), as shown in Fig. 5a, b. This lower degree of

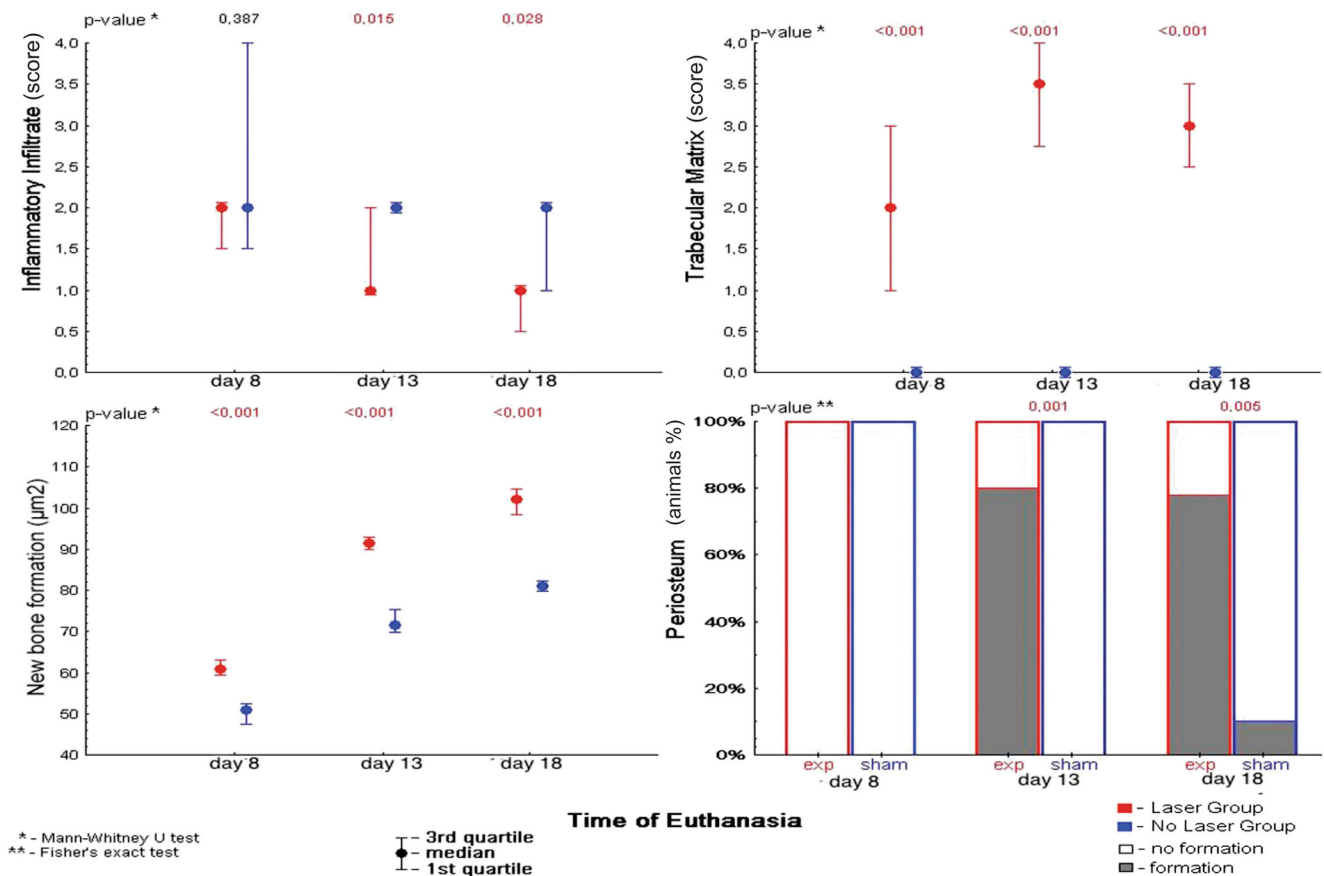


Fig. 3 Morphometric analysis. Similar inflammatory infiltration was observed for LLLT and control rats at day 8 (subgroups A1 and B1). A significant reduction in inflammatory infiltration was only observed for LLLT rats at day 13 (subgroup A2). Trabecular matrix formation was found in all of the LLLT rats (group A). Periosteal formation was not

seen at day 8 in either group (subgroups A1 and B1) but was present in the LLLT rats at days 13 and 18 (subgroups A2 and A3). A significant difference in new bone formation was observed for LLLT rats at all time points ($p < 0.001$)

inflammation was maintained at day 18 (subgroup A3; $p = 0.028$). LLLT rats in subgroups A1, A2, and A3 showed an emergence of trabecular bone formation over time, with significant differences among the three subgroups measured ($p < 0.01$ for all 3 days). In contrast, no trabecular matrix formation was observed for any of the control rats (subgroups B1, B2, or B3). Periosteal formation was not seen in any of the rats after 8 days of healing (subgroup A1 and B1), but a high percentage of animals with periosteal formation were found by day 13 in the LLLT group (subgroup A2) as compared with control rats at the same time point (subgroup B2; $p = 0.001$). This increased periosteal response at day 13 was maintained to day 18 for LLLT rats (subgroup A3) whereas control rats at day 18 had only just started to show periosteal differences (subgroup B3 $p = 0.005$). With regard to bone formation, significant differences were measured among the groups at each time point, with better results identified for LLLT rats (subgroups A1, A2, and A3) as compared with their respective

control counterparts (subgroups B1, B2, and B3; $p < 0.001$ for all periods).

Immunohistochemistry results (Fig. 6) showed higher expression of osteocalcin in the tissue samples from LLLT rats (subgroup A1) at day 8 as compared with that from the control rats at the same time point (subgroup B1; $p = 0.007$). Whereas expression of osteocalcin increased for the control rats by day 13 (subgroup B2), osteocalcin expression remained higher for LLLT rats (subgroup A2). These results indicate that LLLT rats (group A) had an anticipation on bone-remodeling response as compared with control rats (group B). By day 18, rats in both groups showed no changes in osteocalcin expression from day 13. Osteopontin showed the expected behavior (increase on days 8 and 18 and decrease on day 13) in both groups. The difference between the LLLT and the control group was significant only on day 8 ($p = 0.033$). LLLT and control rats showed similar expression changes for osteonectin. Control rats at day 13 (subgroup B2) showed a lower expression of osteonectin as compared with the LLLT rats at that same time point ($p = 0.018$), and no significant

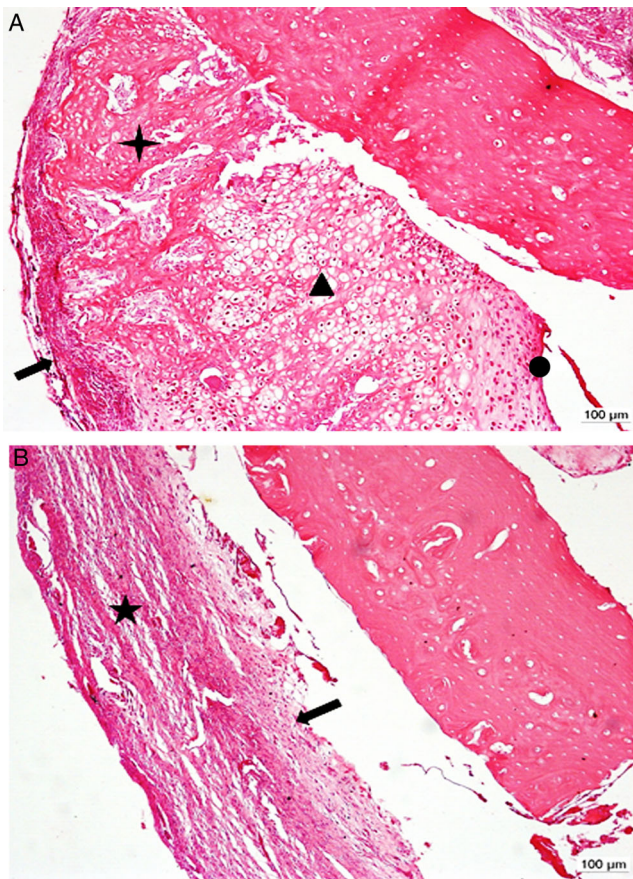


Fig. 4 Histological sections after 13 days. **a** LLLT rats; it is possible to observe trabecular bone matrix formation (*cross*), inflammatory infiltration (*arrow*), chondrocytes presence (*triangle*), and periosteum formation (*sphere*). **b** Control rats; fibroblast re-composition (*star*) and inflammatory infiltration (*thick arrow*) can be observed

difference was observed for osteonectin expression by day 18 between the two groups.

Discussion

When creating a clinical bone fracture model, it is crucial to produce a gap that prevents contact between the bone fragments, as contact might provide a more favorable environment for the union process and facilitate bone growth. Besides this, bone defects of small diameters are not sufficiently reliable to demonstrate the efficacy of lasers as biomodulatory therapies for bone repair [1, 17]. In our model, the stability provided by the plate allowed ambulation and weight bearing [18].

The 808-nm wavelength of the laser used for bone remodeling is within the infrared range and also within the so-called optical window that spans the red and near-infrared wavelengths; this wavelength ensures proper penetration of the laser light into biological tissues. Once light absorption and scattering (which is dependent on the wavelength and its maximal penetration) are obtained in a range between red and

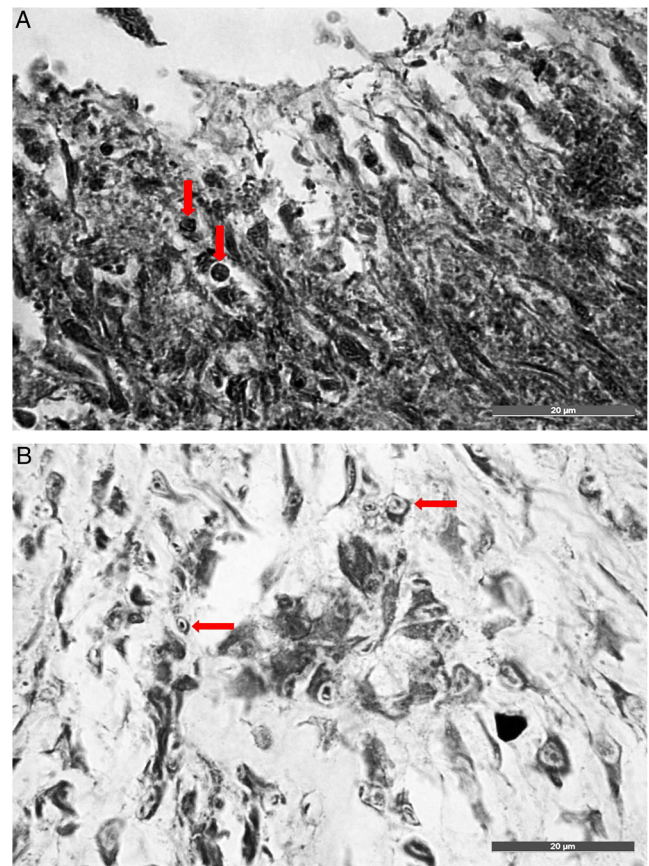


Fig. 5 Inflammatory infiltration cells after 13 days. **a** A score of 1 was found for LLLT rats. **b** A score of 2 was determined for the control rats. The *red arrows* correspond to inflammatory cells

near-infrared lights, this interval will provide the ideal penetration into the biological tissue [5, 19–21]. Indeed, it has been shown that 808-nm light penetrates as much as 54 % deeper than 980-nm light [22].

Real power was chosen to provide the best energy level in the least possible time (5 s) in unrestrained animals, and the choice of this regime was based on previous studies [23–25]. We chose an irradiation spot on the opposite side of the fixed plate to prevent absorption and scattering losses. Furthermore, the use of eight laser irradiation sessions and the dates chosen for killing the animals were defined so as to stimulate and observe bone growth on proliferative process. The time points were chosen based on previous studies, where growth inhibition was observed within a stimulation period longer than 7–8 days after surgery, with evidence of bone formation between 7 and 15 days and a reduction in the rate of bone formation from day 21 [2, 26–28].

The reduction in inflammatory infiltration observed in days 13 and 18 in the LLLT rats led us to assume that these rats were possibly less affected by the inflammatory phase of bone repair, thus allowing for an earlier reparative phase and, consequently, earlier new bone formation, as previously observed [29]. Inflammatory infiltration is part of the bone remodeling

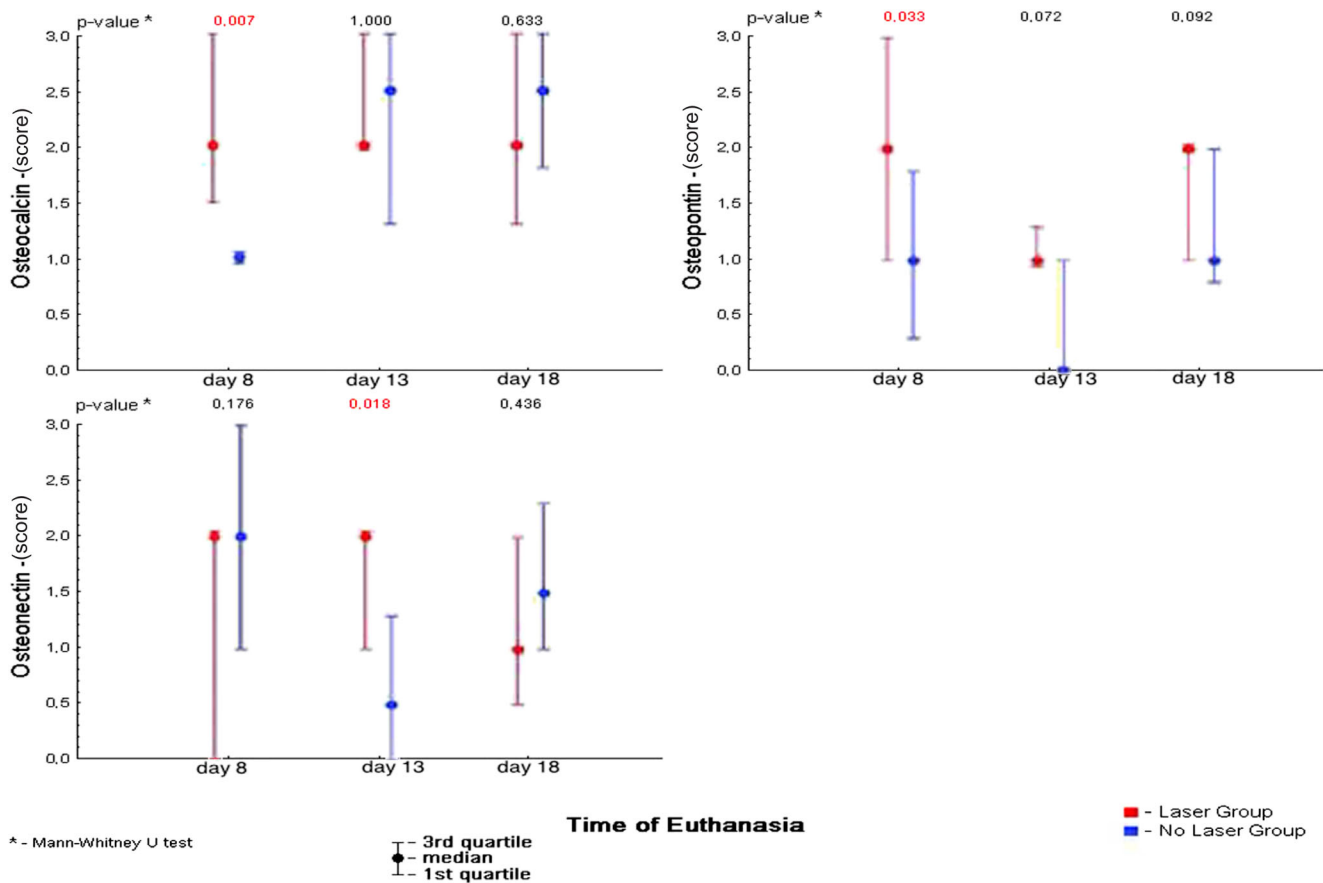


Fig. 6 Immunohistochemical analysis. Osteocalcin and osteopontin were detected early in LLLT rats (group A) with statistical significance observed at day 8 (subgroup A1) as compared with the control rats at that same time point. Osteonectin expression was significantly higher in

LLLT rats at day 13 (subgroup A2), as was periosteum formation. None of the proteins showed any difference in expression at day 18 between the two groups (groups A and B)

process, and it is useful if not drawn out, as longer inflammatory periods compromise the final bone quality. Laser irradiation did not eliminate the inflammation; rather, it expedited all of the steps involved in bone formation, including this inflammatory phase. The reduction in inflammatory infiltration, together with the increase in periosteal development and considerable increase in trabecular matrix formation, showed that rats in the LLLT group underwent an earlier and more organized process of bone formation. In the absence of LLLT, however, no significant trabecular matrix was formed, which is indicative of a slower and less-organized process.

At the cut edge of the fracture, both osteocalcin and osteopontin—two proteins associated with extracellular matrix formation and osteoblast activity [30]—were detected early in LLLT rats, which is consonant with the microscopic results. This is very important, as these matrix factors contribute to the growth, shape, and size of the bone matrix, and affect the quality of the matrix that is produced [31]. Indeed, LLLT and its potent effect on increasing proliferation and cell viability may significantly contribute to many biomedical resources that augment tissue formation and repair in regenerative medicine [32]. Thurner's study [31] on osteopontin

deficiency showed a 30 % decrease in fracture toughness in the absence of the protein, suggesting an important role for osteopontin in impeding crack propagation. Its presence on the surface of samples in “in vivo” bone experiments also suggests its involvement in the process of cell-matrix adhesion, and matrix-matrix modeling and remodeling [33]. Our results also suggest a possible connection between the emergence of osteonectin and the formation of the periosteum, both of which are involved in callus formation. A significant amount of osteonectin during this stage adds to the progress of bone formation, because it incorporates collagen, an important protein required for the acquisition of the tensile strength of the bone. The mineralization and subsequent completion of the repair process of a fracture can be achieved only when proteins that have an affinity for calcium (such as osteocalcin and osteopontin) promote mineral deposition, and those with an affinity for collagen (such as osteonectin) promote bone strength.

Previous studies have investigated the effect of laser therapy on fracture healing [1, 5, 29, 34, 35] using injury models that allow contact between the bone fragments. This led professionals in the field to question the efficacy of LLLT in

conditions that would not be resolved without bone-remodeling aids. Our investigation confirms the beneficial effects of LLLT in fracture healing [36], not only in reducing the inflammatory phase but also in intensifying the reparative phase of repair.

Nonunions represent a treatment challenge for orthopedic surgeons and a serious socioeconomic problem for the patient. Our study provides a solution to these concerns and show that LLLT may be a useful therapeutic tool for bone repair and for the treatment of impaired bone healing in clinical practice.

Limitations

In future studies, we should measure the reduction of the gap using radiological images, to provide some insight into the potential use of LLLT in bone-lengthening surgeries.

Conclusions

We show that LLLT is effective in enhancing bone healing in a rat nonunion femoral fracture model in vivo. LLLT has an effect on all phases of this repair process by increasing the expression of bone formation proteins in vivo and by shortening all phases of bone remodeling.

Ethical approval Animal manipulation was performed in accordance with the animal testing guide (in agreement with the Brazilian Legislation no. 11.794/2008 for Procedures for the Scientific Use of Animals). This randomized controlled experimental study was previously approved by the Research Ethics Committee of Federal University of São Paulo under no. 1101/09.

Conflict of interest All authors have no conflicts of interest.

References

- Oliveira AM, Castro-Silva II, Fernandes GVO, Melo BR, Alves ATNN, Júnior AS, Lima ICB, Granjeiro JM (2014) Effectiveness and acceleration os bone repair in critical-sized rat calvarial defects using low-level laser therapy. *Laser Surg Med* 46(1):61–67
- Carvalho P, Silva I, Reis F, Belchior A, Facco G, Guimarães R, Fernandes G, Denadai A (2006) Effect of 650 nm low-power laser on bone morphogenetic protein in bone defects induced in rat femors. *Acta Cir Bras* 21(suplem 4):63–68
- Claes L, Willie B (2007) The enhancement of bone regeneration by ultrasound. *Prog Biophys Mol Biol* 93(1–3):384–398
- Haal BK (2005) Bones and cartilage: developmental and evolutionary skeletal biology. Academic, San Diego, CA
- Shakouri SK, Soleimanpour J, Salekzamani Y, Oskuie M (2010) Effect of low-level laser therapy on the fracture healing process. *Lasers Med Sci* 25(1):73–77. doi:10.1007/s10103-009-0670-7
- Childs S (2003) Stimulators of bone healing. Biologic and biomechanical. *Orthop Nurs* 22(6):421–428
- Giannunzio GA, Speerli RC, Guglielmotti MB (2008) Electrical field effect on peri-implant osteogenesis: a histologic and histomorphometric study. *Implant Dent* 17:118–126
- Ueda Y, Shimizu N (2003) Effects of pulse frequency of low-level laser therapy (LLLT) on bone nodule formation in rat calvarial cells. *J Clin Laser Med Surg* 21(5):271–277. doi:10.1089/104454703322564479
- Hawkins-Evans D, Abrahamse H (2008) Efficacy of three different laser wavelengths for in vitro wound healing. *Photodermatol Photoimmunol Photomed* 24:199–210
- Marchesano L (2005) Comportamento de marcadores séricos de formação e reabsorção óssea após enxerto autógeno em fissure alveolar congênita: sem e com plasma rico em plaquetas. Doctoral, Universidade Estadual Paulista “Júlio de Mesquita Filho”, Araraquara
- Santa Cruz Biotechnology I (2010) osteocalcin (FL-100): sc-30044
- Santa Cruz Biotechnology I (2010) Osteopontin (LFMb-14): sc-73631
- Santa Cruz Biotechnology I (2010) SPARC (AON-5031): sc-73472 instructions guide
- Suvinil catalog - brick (2014)
- Matkowskyj KA, Schonfeld D, Benya RV (2000) Quantitative immunohistochemistry by measuring cumulative signal strength using commercially available software photoshop and matlab. *J Histochem Cytochem* 48(2):303–311
- Pham N, Morrison A, Schwock J, Aviel-Ronen S, Iakovlev V, Tsao M, Ho J, DW Hedley (2007) Quantitative image analysis of immunohistochemical stains using a CMYK color model. *Diagn Pathol*:2–8
- Martins GL, Puricelli E, Baraldi CE, Ponzoni D (2010) Bone healing after Bur and Er:YAG laser osteotomies. *JOMS* 69(4):1214–1220. doi:10.1016/j.joms.2010.02.029
- Drosse I, Volkmer E, Seitz S, Seitz H, Penzkofer R, Zahn K, Matis U, Mutschler W, Augat P, Schieker M (2008) Validation of a femoral critical size defect model for orthotopic evaluation of bone healing: a biomechanical, veterinary and trauma surgical perspective. *Tissue Eng Part C Methods* 14(1):79–88. doi:10.1089/tec.2007.0234
- Huang Y-Y, Chen AC-H, Hamblin M (2009) Low-level laser therapy: an emerging clinical paradigm.3. doi:10.1117/2.1200906.1669
- Silva Júnior A, Pinheiro A, Weismann MOR, Ramalho L, Nicolau R (2002) Computerized morphometric assessment os the effect os low level laser therapy on bone repair: an experimental study. *J Clin Laser Med Surg* 20(2):83–87
- Abramoff MMF, Pereira MD, Alves MTS, Segreto RA, Guilherme A, Ferreira LM (2014) Low-level laser therapy on bone repair of rat tibiae exposed to ionizing radiation. *Photomed Laser Surg* 32(11):618–626. doi:10.1089/pho.2013.3692
- Hudson DE, Hudson DO, Winger JM, Richardson BD (2013) Penetration of laser light at 808 and 980 nm in bovine tissue samples. *Photomed Laser Surg* 31(4):163–168. doi:10.1089/pho.2012.3284
- Garavello-Freitas I, Baranauskas V, Joazeiro P, Padovani C, Pai-Silva MD, Cruz-Hofling M (2003) Low-power laser irradiation improves histomorphometrical parameters and bone matrix organization during tibia wound healing in rats. *J Photochem Photobiol B Biol* 70(2):81–89
- Freitas I, Baranauskas V, Cruz-Hofling M (2000) Laser effects on osteogenesis. *Appl Surf Sci* 154–155:548–554
- Favaro-Pipi E, Ribeiro DA, Ribeiro JU, Bossini P, Oliveira P, Parizotto NA, Tim C, de Araujo HS, Renno AC (2011) Low-level laser therapy induces differential expression of osteogenic genes during bone repair in rats. *Photomed Laser Surg* 29(5):311–317. doi:10.1089/pho.2010.2841
- Barushka O, Yaakobi T, Oron U (1995) Effect of low-energy laser (He-Ne) irradiation on the process of bone repair in the rat tibia. *Bone* 16(1):47–55

27. Friesen LR, Cobb CM, Rapley JW, Forgas-Brockman L, Spencer P (1999) Laser irradiation of bone: II. Healing response following treatment by CO₂ and Nd:YAG lasers. *J Periodont* 70:75–83
28. Guimarães KB (2006) Fotoengenharia do processo de reparo ósseo induzido pela laserterapia de baixa potência (GaAlAs): estudo em fêmures de ratos. Faculdade de Odontologia, PUCRS, Porto Alegre
29. Giordano V, Knackfuss IG, Gomes RC, Giordano M, Mendonça RG, Coutinho F (2001) Influência do Laser de baixa energia no processo de consolidação da fratura de tibia: estudo experimental em ratos (Influency of low-level laser on healing process of tibial fracture: experimental study in rats). *Rev Bras Ortop* 36(5):174–178
30. Noda M, Denhardt D (2008) Osteopontin. In: AP I (ed) *Principles of bone biology*, 3rd edn, pp 351–366
31. Thurner PJ, Chen CG, Ionova-Martin S, Sun L, Harman A, Porter A, Ager JW, Ritchie RO, Alliston T (2010) Osteopontin deficiency increases bone fragility but preserves bone mass. *Bone* 46:1564–1573. doi:10.1016/j.bone.2010.02.014
32. Abrahamse H (2012) Regenerative medicine, stem cells, and low-level laser therapy: future directives. *Photomed Laser Surg* 30(12):681–682. doi:10.1089/pho.2012.9881
33. Irie K, Zalzal S, Ozawa H, McKee MD, Nanci A (1998) Morphological and immunocytochemical characterization of primary osteogenic cell cultures derived from fetal rat cranial tissue. *Anat Rec* 252(4):554–567. doi:10.1002/(SICI)1097-0185(199812)252:4<554::AID-AR6>3.0.CO;2-2
34. Lirani-Galvão A, Jorgetti V, Silva OL (2006) Comparative study of how low-level laser therapy and low-intensity pulsed ultrasound affect bone repair in rats. *Photomed Laser Surg* 24(6):735–740. doi:10.1089/pho.2006.24.735
35. Tajali SB, MacDermid JC, Houghton P, Grewal R (2010) Effects of low power laser irradiation on bone healing in animals: a meta-analysis. *J Orthop Surg Res* 5:1. doi:10.1186/1749-799X-5-1
36. Park J, Kang K (2012) Effect of 980-nm GaAlAs diode laser irradiation on healing of extraction sockets in streptozotocin-induced diabetic rats: a pilot study. *Lasers Med Sci* 27:223–230